

Intermolecular Potentials of Mean Force of Amino Acid Side Chain Interactions in Aqueous Medium

Sergio A. Hassan*

Center for Molecular Modeling, Division of Computational Bioscience (CMM/DCB/CIT) National Institutes of Health, DHHS, Bethesda, Maryland 20892

Received: July 16, 2004; In Final Form: September 17, 2004

A systematic study of the potentials of mean force (PMF) of hydrogen-bonded amino acid side chains in water is reported. Hydrogen-bonding (HB) partners are classified according to the hybridization state of their donor and acceptor atoms, as well as the net charge of the interacting pairs. This classification leads to a total of 42 classes of representative HB interactions. Constrained molecular dynamics simulations are carried out to calculate the intermolecular mean force (MF) of the solute molecules in an explicit solvent composed of nonpolarizable TIP3P water. Long-range forces are calculated using particle mesh Ewald (PME) summation in a cubic lattice with periodic boundary conditions. The intermolecular PMF are obtained by integrating the MF along a specified reaction path. MF autocorrelation functions and correlation times are calculated for each HB class. Statistical errors in the MF and PMF are estimated and reported. The results are compared with those reported in the literature for simpler systems in the liquid phase. The implications of the results for the description of effective HB interactions in continuum approximations of solvent effects in mesoscopic systems are discussed.

1. Introduction

Hydrogen-bonding (HB) interactions in biological molecules such as proteins and nucleic acids are known to be central to their function.^{1,2} Structural stabilization, dynamics, and thermodynamics of macromolecules are regulated by HB interactions. These may be intra- or intermolecular and may be formed with the surrounding solvent. In water-accessible regions of proteins, the effective strengths of intramolecular HB are modulated by the surrounding polar/polarizable medium that controls electrostatic effects, and by explicit competition with the solvent molecules for available HB. Besides the energetics, the electron density around the donor and acceptor groups also determines a preferable directionality of the interactions.^{3–5} Estimation of the strength and geometry of HB is a difficult task even for small molecular species in the gas phase.⁵ The problem is more challenging in solution or in the solid state where the interaction with the surrounding medium modulates the energy and influences the geometry of the H-bonded species, shifting their average values from those in the gas phase.⁴

Potentials of mean force (PMF) between simple chemical species in the liquid phase have been reported on the basis of analytical techniques and computer simulations.^{6–25} These calculations usually involve small systems such as chloride or sodium ion pairs.^{6–10} More recently, calculations of PMF in larger systems such as guanidine, acetate, and lysine ion pairs have begun to emerge.^{11–13} However, a systematic study of all possible HB interactions between amino acid side chains in an aqueous medium has not been reported. This study is necessary, because unlike covalent bonding, the characteristics of HB interactions are nonadditive and nontransferable even in simple systems.^{2,26–28}

A number of studies^{6–25,29} have shown that PMF obtained from computer simulations are sensitive to the treatment of long-

range electrostatics, cutoff schemes, boundary conditions, and the water model used (e.g., polarizable versus nonpolarizable). Earlier studies showed that for a given system, the number, location, and relative energies of the minima in the potential might differ substantially, depending on the boundary conditions and electrostatic cutoff scheme employed.^{6,8–25,30} Even in a simple system composed of two monovalent ions in water at the dilute solution limit, differences in energies have been reported that are in the range of typical HB interactions in proteins.^{16,21} Nonetheless, computer simulations have a unique advantage over analytical methods and experimental techniques in that the microscopic structure of the solvent around the solutes and its dynamic properties can be analyzed. For example, short-time solvent dynamics, spatial reconfiguration, orientational distribution, cooperative effects, dielectric properties, and intrasolute forces induced by the solvent can be studied in detail.

The extensive calculations performed in this paper quantify the strength of HB in proteins at the theoretical level provided by a molecular mechanics (MM) approximation. HB interactions in an aqueous medium are studied using constrained molecular dynamics simulations in an explicit solvent composed of nonpolarizable TIP3P water molecules.³¹ Periodic boundary conditions^{32,33} (PBC) and particle mesh Ewald (PME) summation^{34–38} are used to calculate the mean force (MF) and the potential of mean force (PMF) between all the representative HB pairs.

The systematic calculations reported herein aim to accomplish the following: (i) quantify the strength of the interactions in solution to obtain information on the position and energy of minima and transition states; (ii) understand the structural and dynamical properties of the solvent around the solute and the origin of the intersolute forces induced by the solvent (cooperativity). Objective i is addressed in this paper, and objective ii will be reported elsewhere. These calculations also provide a quantitative basis for the development of continuum models for solvent effects in mesoscopic systems. In particular, quantifying

* mago@helix.nih.gov.

TABLE 1: Side-Chain Donor and Acceptor Group Classification Based on Chemical Atom Type, Ionization State, and Hybridization

Acceptor Group	
O sp ²	Asn , ^a Gln Asp ⁻ , Glu ⁻
O sp ³	Tyr ^b
N sp ²	Ser , Thr His
S sp ³	Cys, Met
Donor Group	
O sp ²	Tyr
O sp ³	Ser , Thr
N sp ²	His , Arg, ^c Trp His ⁺ Asn , Gln
N sp ³	Arg ⁺ ^d Lys ⁺

^a Representative member of each group is shown in bold. ^b Due to the double-bond character of the CO bond of the hydroxyl group. ^c Neutral NH group. ^d Charged NH₂⁺ group.

the energetics of HB interactions in amino acids is a necessary step toward the development of a continuum approximation in proteins and peptides.^{39–42}

This paper is organized as follows: Section 2 describes the system studied and outlines the computational details; in Section 3, the results are reported and discussed, MF and PMF are calculated, and their standard deviation and statistical error estimates reported; whenever possible, comparison with previous results is provided; in Section 4, a summary is presented, and the implications of these calculations for the development of continuum approximations in macromolecules are briefly discussed.

2. Potentials of Mean Force Calculations

Hydrogen bonding (HB) interactions between side chains of the 20 naturally occurring amino acids may be classified according to hybridization states, the chemical nature of the donor and acceptor atoms, and the charge of the interacting groups.^{3,40} This classification is shown in Table 1, where the representative member of each group is identified in bold.⁴⁰ Interactions involving backbone –CO and –NH groups, classified as O sp² and N sp², respectively, are not studied here.⁴⁰ Only the protonated forms of arginine and lysine and the unprotonated form of aspartate are studied. Both protonated and neutral forms of histidine are considered. This classification yields 6 acceptor and 7 donor groups, resulting in a total of 42 types of HB interactions.

The PMF, $W(\Omega)$, can be defined as the free energy of the system as a function of a selected subset, Ω , of the configuration space, $\Gamma \supset \Omega$. The function $W(\Omega)$ can be calculated from the definition⁴³

$$W(\Omega) = -kT \ln \rho(\Omega) + a \quad (1)$$

where $\rho(\Omega)$ is the conditional probability distribution defined on Ω ; a is a constant. In practice, the numerical calculation of the PMF requires one to evaluate $\rho(\Omega)$ using molecular dynamics or Monte Carlo techniques. However, the inefficient sampling of high-energy regions of the Ω -space using either method can compromise the quality of the results. To improve the sampling and accuracy of the calculations, umbrella sampling^{44–47} was introduced in which an external potential $U(\Omega)$ is added to the Hamiltonian that facilitates the sampling of inaccessible regions of Ω . Although the potential $U(\Omega)$ is not part of the original Hamiltonian, $H(\Omega)$, of the system, the

correct PMF can be obtained using the relation⁴⁸ $W(\Omega) = -kT \ln \rho_u(\Omega) - kTU(\Omega) + kT \ln \langle kTU(\Omega) \rangle_u$, where the index u indicates that the corresponding quantity is calculated with the biased potential (i.e., with a Hamiltonian, $H_u(\Omega) = H(\Omega) + U(\Omega)$). Once the PMF is known, the MF can be calculated from $\mathbf{F} = -\nabla W$.

An alternative way to calculate $W(\Omega)$ is from the definition of potential as the work required to create the system in a configuration $\Omega \subset \Gamma$, from an initial configuration Ω_0 , where the reference of energy, $W(\Omega_0)$, is defined. For the case of two solutes with fixed internal degrees of freedom (rigid bodies) that are brought together preserving their relative spatial orientation, $W(\Omega)$ is given by

$$W(\Omega) = W(\Omega_0) - \int_{\tau} \mathbf{F}(\mathbf{r}) \cdot d\mathbf{r} \quad (2)$$

where Ω_0 and Ω are the initial and final configurations, τ defines the trajectory or reaction path characterized by a vector \mathbf{r} within the volume of the solvent, $d\mathbf{r}$ is the differential displacement along τ , and \mathbf{F} is the mean force acting on the solute at each point \mathbf{r} along the reaction path. In practice, to determine $W(\Omega)$ using eq 2, it is necessary to calculate the mean force at each value of \mathbf{r} and subsequently carry out the integration along τ . The mean force is defined by $\mathbf{F}(\mathbf{r}) = \mathbf{F}_d(\mathbf{r}) + \langle \mathbf{F}_s(\mathbf{r}) \rangle$, where \mathbf{F}_d is the direct force between the two solute molecules and $\langle \mathbf{F}_s \rangle$ is the average force exerted by the solvent. The solvent-induced force $\langle \mathbf{F}_s \rangle$ may be nearly as large in magnitude but opposite in sign from the direct component \mathbf{F}_d . Because of this near-cancellation and sensitivity, physically meaningful results for the sum can only be obtained with high-quality simulations.

Both definitions of $W(\Omega)$ have traditionally been used to calculate PMF in simple systems.^{7–13,49–51} In certain cases, eq 1 may be more practical given the availability of standard techniques to recover $W(\Omega)$ from the biased sampling.⁵² Equation 2, however, is more useful when the trajectories generated in the simulations are used not only for calculating $W(\Omega)$ but also to quantify other system properties as well, such as the dynamics of the solvent or its microscopic structure around specific solute configurations. This definition may also be useful in practice for the optimization of HB interactions in continuum models where control of the relative orientation of the interacting pair is required in the parametrization procedure.^{39,40}

In the calculations reported here, the constraints imposed on the solutes apply not only to the intermolecular distance, which is sufficient for isotropic systems,^{7–9} but also to their relative orientation (e.g., see ref 49). In addition, the solute molecules are fixed in space and not allowed to move within the unit cell. Each molecule was built with CHARMM⁵³ and independently minimized in a vacuum. From ab initio and experimental studies of small molecules in the gas phase, the geometrical characteristics of HB have been identified.^{5,26} Typically, the shared proton is oriented toward the lone pair orbitals in the acceptor atom, whereas the angle A···H–D at the shared proton is close to 180° (A = proton acceptor; D = proton donor). These rules also apply in the solid state, although the crystal field produces local perturbations creating a broader distribution of angles and distances than in the gas phase.^{3,4} Quantum mechanical calculations of HB interactions in small organic molecules in an explicit aqueous medium are severely hampered by the computational requirements.^{54,55} By following previous work,⁴⁰ the relative orientations of each pair were determined here by the geometrical rules just described. The amino and carboxy termini of each amino acid were capped with uncharged groups, as reported earlier.⁴⁰ The initial proton–acceptor distance, $r_{\text{H–A}}$,

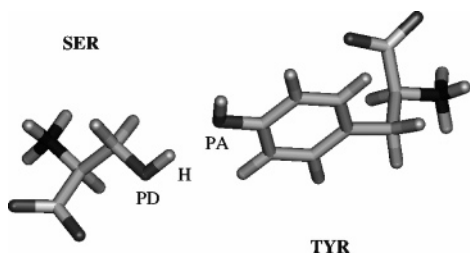


Figure 1. Serine (donor) and Tyrosine (acceptor) in their initial relative conformations. The molecules are capped with artificially uncharged $-\text{NH}_3$ and $-\text{CO}_2$ groups;⁴⁰ this provides for a more realistic representation of the protein environment by excluding solvent without introducing additional charges.

(hereafter denoted by r) was set to $r = 1.0 \text{ \AA}$. The donor molecule was then rigidly rotated about the axis determined by the line $\text{A}\cdots\text{H}-\text{D}$ to find the relative conformation of minimum energy. This protocol was used earlier⁴⁰ and defines a recipe for reproducing the simulation setup. Figure 1 shows the pair Tyr-Ser in its initial conformation. The distance r was then progressively increased in steps of $\Delta r = 0.2 \text{ \AA}$, up to a maximum r_m . The value of r_m is defined as the distance where the magnitude of the mean force, F , as defined here, remained within the estimated statistical error, σ_F , in the interval $(r_m - s) < r < r_m$; with $s = 1 \text{ \AA}$, it was found that $10 < r_m < 14 \text{ \AA}$, depending on the interacting pairs. At $r = r_m$, the intermolecular energy $W(\Omega_0)$ in eq 2 was set to the value of the interaction energy, $W(r_m)$, in a homogeneous dielectric medium with $\epsilon = 78.4$ (i.e., the measured static dielectric permittivity of bulk water at the simulation temperature, $T = 298 \text{ K}$). The intermolecular PMF were calculated using MD simulations of the solvent only, at a fixed solute conformation. Thus, for each value r , the constraints were applied to the internal geometry of the molecules and to their relative angular orientations. The force due to the solvent was calculated as $\langle \mathbf{F}_s(\mathbf{r}) \rangle = \langle \mathbf{r}' \cdot \Delta \mathbf{F}(\mathbf{r}) \mathbf{r}' / 2 \rangle$, where \mathbf{r}' is a unit vector along the direction of movement, and $\Delta \mathbf{F}(\mathbf{r}) = \mathbf{F}_A(\mathbf{r}) - \mathbf{F}_D(\mathbf{r})$, where \mathbf{F}_i is the average force that the solute exerts on the proton acceptor ($i = \text{A}$) or donor ($i = \text{D}$) molecules evaluated at their centers of mass.⁷⁻⁹

Each pair was immersed in a cubic box containing pre-equilibrated TIP3P³¹ water at $T = 298 \text{ K}$. The all-atom (PAR22) representation⁵⁶ of the CHARMM⁵³ force field (version c30) was used. A relatively large solvent box of volume $(46 \text{ \AA})^3$ was used for the unit cell containing ~ 3500 water molecules with a density close to 1 g/cm^3 . This cell size ensures that the minimum-distance image criterion is satisfied for all values of r . In the initial configuration, all water molecules within a distance of 1.4 \AA from any atoms of the solute were removed. During the simulations, the molecules were moved away from each other along one of the main diagonals of the box and along the line $\text{A}\cdots\text{H}-\text{D}$. Because of the noticeable dependence of the results upon the treatment of long-range electrostatics, PME summation^{34-38,57} was used. Theoretical studies have reported on the effects of the Ewald parameters on the calculations of forces.⁵⁸ An appropriate choice of parameters is essential for reliable results. The parameters used in this work are suggested as appropriate within the PME implementation in CHARMM for the system setup used here,⁵⁸ and were specified as follows: width of Gaussian function for summation on reciprocal space, $\kappa = 0.34$; number of grid points for fast Fourier transform of the charge mesh, FFT = 48 in each direction; complimentary error functions calculated with B-spline interpolation of fifth degree (order six); number of unit-cell images added in each direction, $k = 5$. To keep the system electrically neutral, a Cl^- or Na^+ ion was introduced when necessary by

replacing an arbitrary water molecule located far from the solute. The ions were fixed in space throughout the simulations to prevent them from perturbing the solvent molecules that surround the solutes. A shift function was used to shut off the nonbonded interactions at 12 \AA ; a 14-\AA cutoff was used for the nonbonded list update. Water O-H bond lengths were kept fixed using the SHAKE facility in CHARMM, and a 2-fs time step was used for the calculations of forces with a Verlet integration algorithm. The whole system (i.e., the solute plus the pre-equilibrated water) was initially equilibrated for 500 ps. Each time the intermolecular distance r was updated, an equilibration of 40 ps followed to relax local perturbations of the solvent environment. When the system reached a new equilibrium, a 60-ps MD simulation was generated, and data collected every 0.1 ps for analysis. Each simulation comprised an average of 5 ns and took about 1.2×10^3 CPU-hours in a single processor of a Beowulf cluster. The duration of the production phase was chosen as a compromise between CPU time and the statistical error, σ_F , in the MF, which determines the uncertainty of the potential (cf. Section 3). Because of the relative complexity of the solute molecules, an estimation of statistical errors is reported. No attempt was made to evaluate errors from other sources (e.g. systematic errors due to the approximation

$$W(r_m) \approx - \int_{\infty}^{r_m} F(r) dr;$$

or hysteresis effects). The error of $F(r)$ is calculated as $\sigma_F = s_F/N_u^{1/2}$, where s_F is the standard deviation of $F(r)$ obtained from the fluctuating force $F(r, t)$; N_u is the number of uncorrelated steps, given by $N_u = \tau/t_c$, where τ is the total time of the simulation for each r ; t_c is the autocorrelation time of $F(r)$ (cf. Section 3). The normalized MF autocorrelation function C_F is defined by $C_F(r, t) = \tau^{-1} s_F^{-2} \int [F(r, t')F(r, t+t') - \langle F(r) \rangle^2] dt'$, and its discretized version is used in the actual calculations. The statistical error σ_W in the potential was estimated numerically from $\sigma_W^2(r) = \sum [\sigma_F(r)\Delta r]^2$.

3. Results

Figure 2 shows the intermolecular PMF for all of the acceptor-donor pairs obtained from the classification given in Table 1. The reaction coordinate r is defined along the straight line that connects the three atoms $\text{A}\cdots\text{H}-\text{D}$. The potentials show, nearly in all cases, a well-defined contact minimum $W(r) = W_c$ at $r = r_c$, and a more shallow solvent-separated minimum $W(r) = W_{ss}$ at $r = r_{ss}$. In general, W_c is lower than W_{ss} , with $W_{ss} - W_c > kT$, except for three cases involving Cys as the acceptor group and a charged group as the donor: $W_c - W_{ss} \approx 0.2 \text{ kcal/mol}$ (Arg^+), $W_c - W_{ss} \approx 0.9 \text{ kcal/mol}$ (His^+), $W_c - W_{ss} \approx 1.6 \text{ kcal/mol}$ (Lys^+); for the pair Asn-Lys⁺, both minima are equally stable within the statistical uncertainty. The contact minima are, in general, global minima of the potential except for the three cases involving Cys mentioned already and for the pair His⁰-Asn. Note, however, that W_{ss} for Cys interacting with His⁺, and possibly with Arg⁺, becomes the global minimum of $W(r)$. The PMF show that Cys-Lys⁺ and His⁰-Asn are actually unstable species in the solvent, with two metastable states at the contact and solvent-separated minima. An energy barrier $W(r) = W_t$ at a distance $r = r_t$ separating both local minima is present in all cases. Activation energies, $\Delta W = W_t - W_c$, range from 1.5 kcal/mol for Cys-Lys⁺ to 6.2 kcal/mol for Ser-His⁺. As a rule, Ser acting as an acceptor shows the largest values of ΔW regardless of its donor partner, whereas Cys shows the lowest ΔW . A summary of the positions and energies of the transition states and the two local minima are

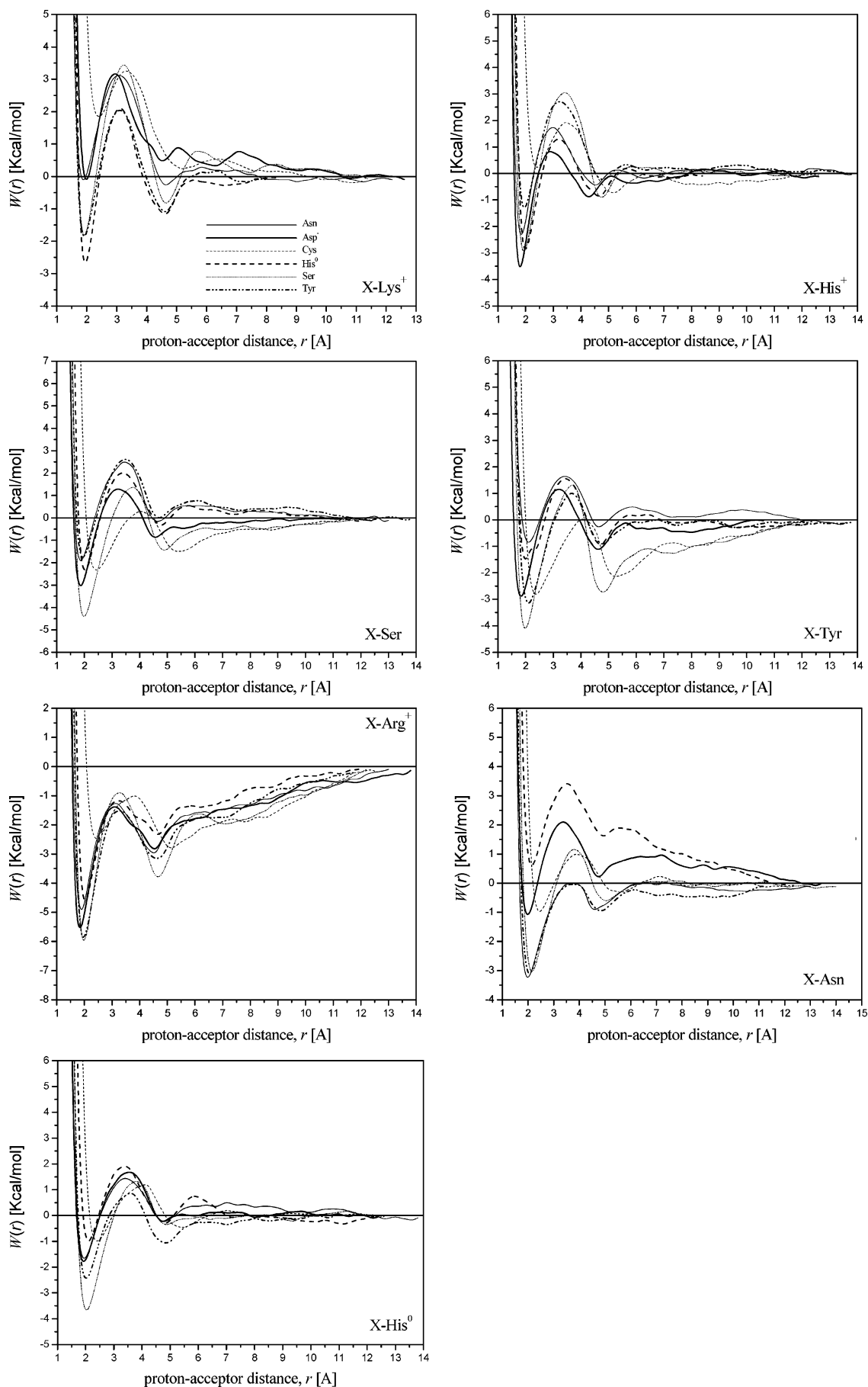
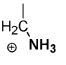
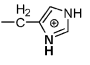
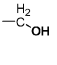
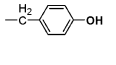
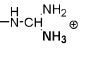
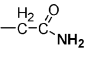
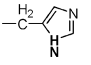


Figure 2. Potentials of mean force, $W(r)$, for all the HB classes obtained from Table 1. Label X denotes one of the acceptor molecules shown in the inset of panel X-Lys⁺ (upper-left). Positions and energies of the minima and transition states are summarized in Table 2. Approximating B-spline curves were used to smooth the potentials for visualization purpose.

TABLE 2: Position^a and Energy^b Values of the Minima and Transition States of the Potentials of Mean Force $W(r)$'s Shown in Figures 2

		DONOR GROUPS							
		Lys ⁺	His ⁺	Ser	Tyr	Arg ⁺	Asn	His ⁰	
									
ACCEPTOR GROUPS	Asn	-0.2 (0.3) 3.2 (0.3) -0.2 (0.3) 1.8; 3.0; 4.6	-2.7 (0.3) 1.8 (0.3) -0.5 (0.3) 1.8; 3.0; 4.6	-2.1 (0.3) 2.7 (0.3) -0.1 (0.2) 1.8; 3.4; 4.6	-0.8 (0.3) 1.8 (0.3) -0.2 (0.3) 2.0; 3.4; 4.6	-5.0 (0.3) -1.1 (0.3) -2.9 (0.3) 1.8; 3.2; 4.6	-3.3 (0.3) 0.1 (0.2) -0.8 (0.2) 2.0; 3.6; 4.6	-1.7 (0.3) 1.5 (0.3) -0.3 (0.3) 2.0; 3.4; 4.8	W_c (ΔW_c) W_t (ΔW_t) W_{ss} (ΔW_{ss}) $r_c; r_t; r_{ss}$
	Asp ⁻	-0.3 (0.4) 3.3 (0.4) 0.6 (0.4) 2.0; 3.0; 4.4	-3.9 (0.4) 0.9 (0.4) -0.9 (0.3) 1.8; 2.8; 4.2	-3.2 (0.4) 1.4 (0.3) -0.8 (0.3) 1.8; 3.2; 4.6	-3.0 (0.3) 1.3 (0.3) -1.0 (0.3) 1.8; 3.2; 4.6	-5.9 (0.4) -1.4 (0.4) -2.9 (0.4) 1.8; 3.2; 4.6	-1.1 (0.4) 2.2 (0.3) 0.3 (0.3) 2.0; 3.4; 4.8	-1.8 (0.4) 1.7 (0.3) -0.3 (0.3) 1.8; 3.6; 4.8	W_c (ΔW_c) W_t (ΔW_t) W_{ss} (ΔW_{ss}) $r_c; r_t; r_{ss}$
	Cys	1.9 (0.3) 3.4 (0.3) 0.3 (0.2) 2.4; 3.4; 5.2	0.1 (0.3) 2.0 (0.3) -0.8 (0.3) 2.4; 3.4; 5.2	-2.3 (0.2) 0.4 (0.2) -1.4 (0.2) 2.4; 4.0; 5.4	-2.8 (0.3) 0.2 (0.2) -2.1 (0.2) 2.4; 4.0; 5.2	-2.6 (0.3) -1.0 (0.3) -2.8 (0.3) 2.4; 3.8; 5.2	-1.0 (0.2) 1.1 (0.2) -0.3 (0.2) 2.4; 3.8; 5.6	-1.1 (0.3) 1.2 (0.2) -0.5 (0.2) 2.4; 4.2; 5.4	W_c (ΔW_c) W_t (ΔW_t) W_{ss} (ΔW_{ss}) $r_c; r_t; r_{ss}$
	His ⁰	-2.7 (0.2) 2.2 (0.2) -1.1 (0.2) 2.0; 3.2; 4.6	-3.1 (0.3) 1.4 (0.2) -0.8 (0.2) 2.0; 3.2; 4.6	-2.6 (0.3) 2.0 (0.3) -0.4 (0.2) 2.0; 3.4; 4.8	-1.6 (0.3) 1.7 (0.3) -0.8 (0.2) 2.0; 3.4; 4.8	-4.8 (0.3) -1.1 (0.3) -2.3 (0.3) 2.0; 3.2; 4.6	0.6 (0.3) 3.5 (0.3) 1.7 (0.2) 2.2; 3.6; 5.0	-1.2 (0.3) 1.9 (0.3) -0.4 (0.3) 2.0; 3.4; 4.8	W_c (ΔW_c) W_t (ΔW_t) W_{ss} (ΔW_{ss}) $r_c; r_t; r_{ss}$
	Ser	-1.9 (0.3) 3.6 (0.3) -0.8 (0.2) 1.8; 3.2; 4.6	-3.1 (0.3) 3.1 (0.3) -1.0 (0.3) 2.0; 3.4; 4.8	-4.6 (0.3) 1.4 (0.2) -1.5 (0.2) 2.0; 3.8; 4.8	-4.2 (0.3) 1.5 (0.3) -2.7 (0.2) 2.0; 3.8; 4.8	-6.2 (0.3) -0.9 (0.3) -3.9 (0.3) 2.0; 3.2; 4.6	-3.0 (0.3) 1.3 (0.2) -0.5 (0.2) 2.2; 3.8; 5.0	-3.9 (0.3) 1.4 (0.3) -0.4 (0.3) 2.0; 3.8; 4.8	W_c (ΔW_c) W_t (ΔW_t) W_{ss} (ΔW_{ss}) $r_c; r_t; r_{ss}$
	Tyr	-1.9 (0.2) 2.2 (0.2) -1.1 (0.2) 1.8; 3.2; 4.6	-1.4 (0.3) 2.8 (0.3) -0.2 (0.3) 2.0; 3.2; 4.8	-1.8 (0.3) 2.7 (0.3) 0.1 (0.3) 2.0; 3.6; 4.6	-3.1 (0.3) 1.1 (0.3) -0.9 (0.3) 2.0; 3.6; 4.8	-5.9 (0.3) -1.3 (0.3) -3.0 (0.3) 2.0; 3.4; 4.6	-3.2 (0.2) 0.1 (0.2) -0.9 (0.2) 2.0; 3.8; 4.8	-2.6 (0.3) 0.9 (0.2) -1.1 (0.2) 2.0; 3.6; 4.8	W_c (ΔW_c) W_t (ΔW_t) W_{ss} (ΔW_{ss}) $r_c; r_t; r_{ss}$

^a In angstroms; errors $\Delta r \approx 0.1 \text{ \AA}$ for all distances reported. ^b In kcal/mol; errors in parentheses ($\Delta W \equiv \sigma_W$). W_c , W_{ss} , and W_t denote the energies at the contact minimum, at the solvent-separated minimum, and at the transition state, respectively; r_c , r_{ss} , and r_t are the corresponding positions of the minima and transition states measured as a function of the proton-acceptor distance r . Only functional groups of the interacting molecules are shown.

shown in Table 2, along with their statistical error estimates. The potentials of some of the pairs show additional barriers and local minima at positions $r > r_{ss}$, that are not shown in Table 2 and will not be discussed here. Some of these barriers are relatively high, as in the cases of Ser-Lys⁺ or His⁰-His⁰ pairs, with activation energies of ~ 1.7 and ~ 1.0 kcal/mol, respectively. These oscillations in $W(r)$ seem to originate in a further structural rearrangement of water molecules around the solutes. A detailed study of the structural and dynamical properties of the solvent that determine the shape of $W(r)$ will be reported elsewhere. Table 2 shows that the stronger interactions usually involve Arg⁺ as the acceptor group; on the other hand, Lys⁺ displays relatively weak interactions with its acceptor partners, despite its ionic character. In particular, the pair Lys⁺-Asp⁻ ranks among the least stable species, being about 2.5 kcal/mol less stable than Lys⁺-His⁰, for example, presumably because of the favorable solvation of the molecules.

A direct comparison with previously reported PMF of similar systems is not straightforward because of the noticeable sensitivity of the results to the different simulation protocols, the treatment of the long-range interactions, the size of the solute, and the water model used. The PMF are also sensitive to the initial relative orientation of the interacting pairs. In a recent study,¹² PMF of small side-chain analogues were reported. One of the initial orientations of the pair Lys⁺-Glu⁻ is

comparable to the orientation of the Lys⁺-Asp⁻ system studied here. In that study, the contact minimum was found to be a global minimum of the PMF with energy $W_c \approx -1$ kcal/mol. Although error bars were not reported, this bound state seems to be ~ 0.7 kcal/mol more stable than that obtained here, $W_c = -0.3 \pm 0.4$ kcal/mol (cf. Table 2). A larger discrepancy is found at the solvent-separated minimum, $W_{ss} \approx -0.5$ kcal/mol in ref 12 versus $W_{ss} = +0.6 \pm 0.4$ kcal/mol in this study. Also of interest is the comparison of the PMF between the pair Asp⁻-His⁺ obtained here and the analogue of the pair His⁺-Glu⁻ in ref 12. Both studies agree on the energies of the transition and the solvent-separated states: $W_t = +0.9 \pm 0.4$ and $W_{ss} = -0.9 \pm 0.3$ kcal/mol (cf. Table 2) versus $W_t \approx +1$ and $W_{ss} \approx -1$ kcal/mol, respectively. However, the energy at the contact minimum was found in ref 12 to be ~ 3 kcal/mol less stable than the value reported in Table 2. For the case of Asp⁻-His⁰, the comparison shows that the energies of both minima are reasonably similar in both studies, although slightly more stable in this study: $W_c = -1.8 \pm 0.4$ and $W_{ss} = -0.3 \pm 0.3$ kcal/mol (cf. Table 2) versus $W_c \approx -2.5$ and $W_{ss} \approx -1$ kcal/mol. However, the transition state was found to be ~ 1.5 kcal/mol more stable in ref 12 than reported in Table 2. Therefore, the contact minimum in the PMF obtained here for Asp⁻-His⁰ is ~ 2 kcal/mol less stable than that for the Asp⁻-His⁺ pair, in contrast to the findings in ref 12. No attempt was made here to

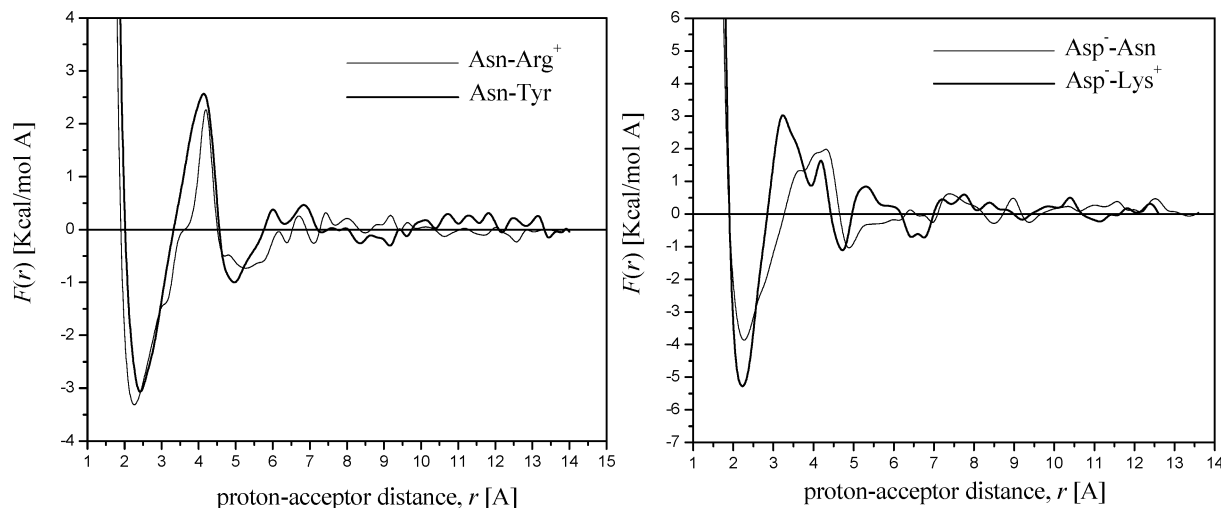


Figure 3. Mean force, $F(r)$, of four representative H-bonded pairs displaying different combinations of charge.

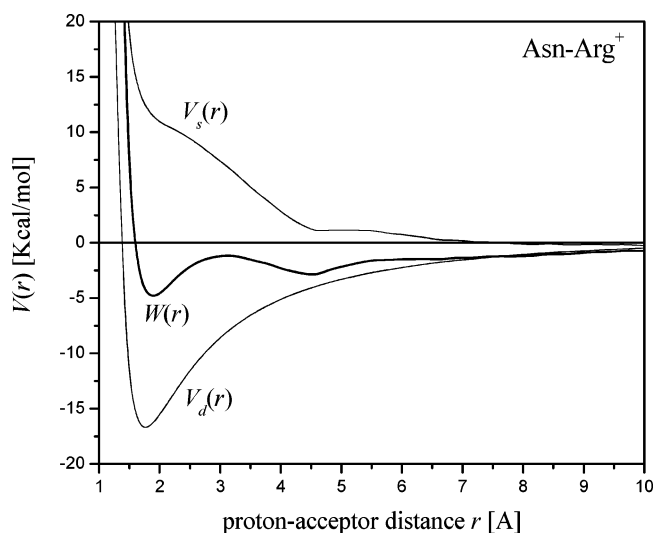


Figure 4. Decomposition of the potential of mean force, $W(r)$, in the direct, $V_d(r)$, and solvent-induced, $V_s(r)$, components, for the Asparagine (acceptor) and Arginine (donor) pair.

identify the origin of these differences, although the treatment of long-range forces may play a role.¹³

Figure 3 shows typical mean-force plots obtained from the simulations, involving different combinations of charge. Figure 4 shows the decomposition of the PMF, $W(r) = V_d(r) + V_s(r)$, in the direct, $V_d(r)$, and the solvent-induced, $V_s(r)$, components, for the pair Asn-Arg⁺. The solvent exerts mainly a repulsive force between the molecules at short distances, although oscillations can be observed at distances larger than r_{ss} (cf. Figure 2). The magnitude of the fluctuations of the mean force varies with the interparticle distance r . For all of the pairs, the standard deviations, s_F^2 s, of $F(r)$ become smaller as r decreases, and remain relatively stable for $r > r_{ss}$. Figure 5 shows s_F as a function of r for the pairs Asp⁻-Arg⁺ and Tyr-Asn. At short distances ($r < r_{ss}$), s_F drops by $\sim 1-2kT/\text{Å}$ when compared to its values at longer distances ($r > r_{ss}$). The largest fluctuations are observed for the ionic pair Asp⁻-Arg⁺ for $r > r_{ss}$ ($s_F \approx 10kT/\text{Å}$); the smallest fluctuations are observed in Asn-Arg⁺ for $r < r_{ss}$ ($s_F \approx 4kT/\text{Å}$). Similar values of mean-force fluctuations were observed in simpler systems, such as in the Na⁺-Cl⁻ pair, with standard deviations in the range 4–10kT/Å.^{7,8} Figure 6 shows the MF autocorrelation functions $C_F(t)$ along with the estimated correlation times t_c for three systems at three representative distances: $r_t < r < r_{ss}$ (Cys-Asn), $r \approx r_{ss}$ (Tyr-

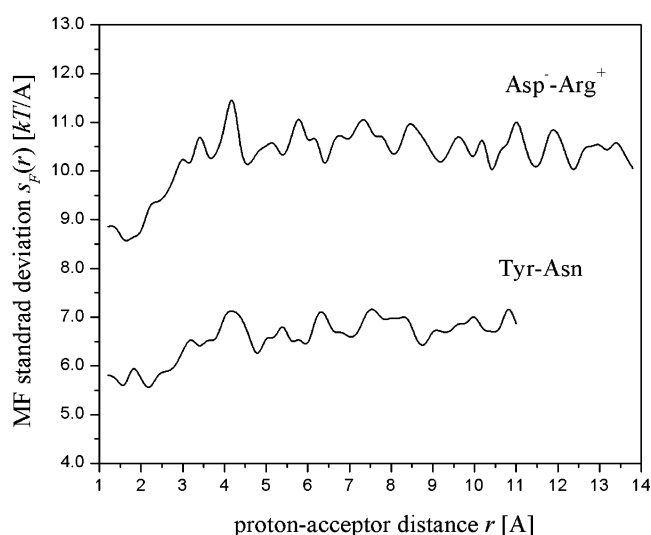


Figure 5. Standard deviations, $s_F(r)$, of the fluctuating intermolecular force, $F(r,t)$, as a function of the proton-acceptor distance r . These plots represent two extreme cases of large and small force fluctuations observed in the simulations.

Tyr), and $r > r_{ss}$ (Asp⁻-His⁰). As a general rule, the solvent dynamics display a high degree of randomness at all distances, with correlation times in the sub-picosecond range, as shown in panel a of Figure 6 for $r = 6 \text{ Å}$. For $r > r_{ss}$, correlation times are smaller than 0.1 ps (i.e., complete randomization occurs within 50 integration steps of the simulation for all pairs). Therefore, statistical errors in the range $\sigma_F \approx 0.2-0.4kT/\text{Å}$ are obtained, depending on the magnitude of the fluctuations. Some exceptions occur, however, where a relatively high degree of force autocorrelation is observed at shorter distances, usually in the range $r_c < r < r_{ss}$, where the solvent is more structured around the solute (unpublished results). In these cases, correlation times may reach the picosecond range. Panel b of Figure 6 displays $C_F(t)$ for two systems that show the highest mean force autocorrelation at short distances, with $t_c \approx 1-2 \text{ ps}$ (the correlation time drops sharply to $\sim 0.1 \text{ ps}$ for $r > r_{ss}$). In these cases, statistical error estimates are in the range $\sigma_F \approx 0.6-1.4kT/\text{Å}$. Note also that similar error bars ($\sigma_F \approx 0.5-0.8kT/\text{Å}$) were obtained in a simpler system composed of two interacting ions.^{7,8} The values obtained here are an acceptable compromise between computing time and accuracy. Propagation to the PMF yields error estimates that are a fraction of kT (cf. Table 2), allowing statistically meaningful conclusions to be drawn. These

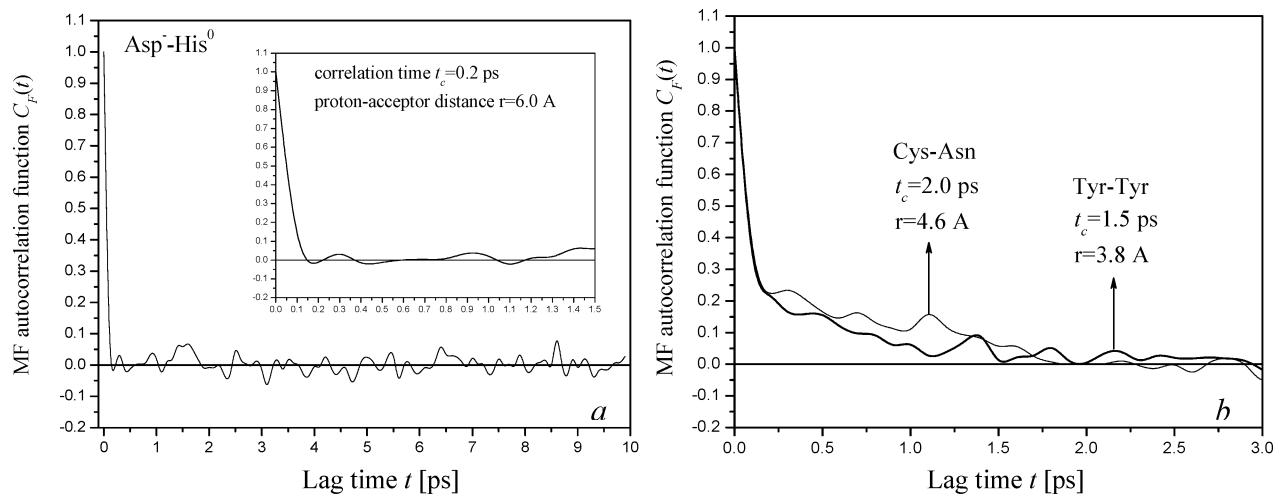


Figure 6. Typical plots of the mean force autocorrelation functions, $C_F(t)$, obtained in the simulations: (a) fast decay observed at distances $r > r_{ss}$; the mean force rapidly randomizes in the subpicosecond time-scale (correlation times $t_c \approx 0.1$ – 0.2 ps); (b) slower decays corresponding to more correlated dynamics, typically observed at distances $r_c < r < r_{ss}$; in these cases t_c is in the range 1–2 ps, although smaller values are observed. B-spline smoothing was used for visualization purpose.

errors are usually in the range $\sigma_W \approx 0.2$ – 0.4 kcal/mol, measured at the contact and solvent-separated minima and at the transition states. The largest errors are observed for the interactions between charged species (i.e., Asp^- with Lys^+ , Arg^+ and His^+) and the largest values are obtained at shorter distances, as expected. In all but two cases, the error bars allow an unambiguous determination of the relative energy of the minima. The exceptions are Asn-Lys^+ and Cys-Arg^+ , where the global minimum could not be identified.

4. Summary and Discussion

A systematic study of the intermolecular PMF of representative HB interactions in proteins has been reported. The short-term goals of these calculations are twofold: (i) to quantify the strength of the interactions in solution and determine the positions and energies at the minima and transition states and (ii) to gain insight into the microscopic structure and dynamics of water molecules around specific solute conformations. Objective i was reported in this paper; objective ii will be reported elsewhere. The long-term goal is to quantify the energetics of HB interactions and the nature of the solvent-induced intersolute forces, as a step toward the development of a realistic continuum model of solvent effects in mesoscopic system such as biomolecules.

In the study reported here, HB partners were classified according to the net charge of the interacting molecules and the hybridization state of the donor and acceptor atoms. The calculations were carried out in an explicit solvent using the TIP3P nonpolarizable water model. Holonomically constrained molecular dynamics simulations were used to estimate the PMF in all cases. The intermolecular MFs between the two solutes were first calculated and the potential obtained by integrating the work along a predefined reaction path. A large body of theoretical work has been reported on the sensitivity of PMF to the treatment of long-range forces, cutoff schemes, and boundary conditions employed^{6–25,29,34–38,57,58}. To build on these earlier studies, an effort was made here to optimize the computational setup within the scope of the available resources. MF autocorrelation functions and correlation times were calculated and reported. In most cases, the dynamics rapidly randomizes the fluctuating force within 0.1 ps. However, correlation times of up to 2.0 ps were found in some cases.

This higher correlation was generally observed between the contact and solvent-separated minima. In this interval, the solvent appears relatively more structured around the solute than it is in bulk (unpublished results). Statistical errors in the MF and PMF were estimated and found acceptable to provide meaningful data and allow unambiguous comparison of relative energies.

The results reported here are relevant in continuum approximations of solvent effects in peptides and proteins. Despite the enthalpic cost required to remove a polar group from a polar solvent, many polar side chains and peptide groups are buried in the interior of proteins.^{59,60} Almost invariably, these groups form internal HB with other buried groups, providing a favorable stabilization that partially compensates the unfavorable desolvation enthalpy.^{60,61} The extent of the net stabilization provided by these interactions has been controversial. Theoretical estimates have been inconclusive^{60,62,63}, whereas experiments seem to suggest that burying a polar group may actually contribute more to protein stabilization than burying a nonpolar group.^{60,64} Quantifying these effects is important from a theoretical perspective: A deficient description of the delicate balance between the unfavorable desolvation and favorable stabilization due to the formation of HB may lead to an incorrect estimation of many biophysical properties such as protein–protein and protein–ligand interactions, protein folding/unfolding, and structure prediction. Dynamical properties can also be adversely affected, leading to inaccurate estimations of important thermodynamic quantities such as transition rates and binding free energies.

Continuum approximations involve the removal of all or some of the solvent molecules and the retention of their effects on the remaining part of the system, usually the solute of interest^{39,41–43,65–69}. Removing the solvent, however, eliminates a number of effects that must be properly described for physically realistic results.^{41,42} Among these effects are bulk electrostatics, hydrophobicity, solvent-induced intrasolute interactions (cooperative effects), HB competition with water molecules, density fluctuations, electrostriction, pressure, and viscosity. An explicit representation of the solvent automatically accounts for these effects. On the other hand, a continuum representation requires each of these effects to be properly described, either by a theoretical model or computational

algorithm (e.g., Langevin dynamics⁸⁹). Depending on the system of interest and the properties to be studied, one or more of these effects may be dominant. In biologically active macromolecules, solvent effects seem to be dominated mainly by electrostatics,^{68–70} hydrophobicity,^{71,72} and hydrogen-bonding^{2,3,73} interactions, all of which have been intensively studied in various contexts. Still, practical and conceptual difficulties remain in quantifying these effects.^{49,60,61,74–82} To address some of these problems, a continuum approximation based on the theory of polar liquids^{83–88} has been proposed to describe electrostatic effects in proteins.^{39–42} The solvent molecules are described by dipoles that reorient and further polarize due to the field created by the solute, and are subjected to thermal fluctuations. The approach makes the transition from a microscopic to a mesoscopic description by taking statistical averages of the microscopic field in the solvent. As discussed previously, a continuum approximation derived from bulk properties requires a close inspection of the resulting strength of HB interactions.^{40,89} This is so, because both the formulation and parametrization of the model invoke neither explicit intrasolute HB interactions nor modulation due to explicit HB competition with the solvent. Therefore, the strength of the interactions that results from such formulations should be carefully reevaluated.⁴⁰ The PMF results reported in this paper can be used to guide this quantitative optimization;⁴⁰ preliminary studies based on this calibration will be reported elsewhere.⁸⁹ It is finally noted that a realistic continuum formulation should also describe transition states energies in the PMF. These energy barriers are important in kinetic processes, and the results reported here may be relevant for this task.⁹⁰

Acknowledgment. The author thanks Peter Steinbach, Bernard Brooks, and Charles Schwieters for useful discussions. This study utilized the high-performance computational capabilities of the Beowulf PC/Linux cluster at the National Institutes of Health, Bethesda, Maryland (<http://biowulf.nih.gov>).

References and Notes

- (1) Pauling, L. *The Nature of the Chemical Bond*; Cornell University Press: Ithaca, New York, 1960.
- (2) Jeffrey, G. A.; Saenger, W. *Hydrogen Bonding in Biological Structures*; Springer-Verlag: Heidelberg, 1991.
- (3) Baker, E. N.; Hubbard, R. E. *Prog. Biophys. Mol. Biol.* **1984**, *44*, 97.
- (4) Murray-Rust, P.; Glusker, J. P. *J. Am. Chem. Soc.* **1984**, *106*, 1018.
- (5) Legon, A. C.; Millen, D. J. *Acc. Chem. Res.* **1987**, *20*, 39.
- (6) Bader, J. S.; Chandler, D. *J. Phys. Chem.* **1992**, *96*, 6423.
- (7) Ciccotti, G.; Ferrario, M.; Hynes, J. T.; Kapral, R. *Chem. Phys.* **1989**, *129*, 241.
- (8) Guardia, E.; Rey, R.; Padro, J. A. *Chem. Phys.* **1991**, *155*, 187.
- (9) Guardia, E.; Rey, R.; Padro, J. A. *J. Chem. Phys.* **1991**, *95*, 2823.
- (10) Friedman, R. A.; Mezei, M. *J. Chem. Phys.* **1995**, *102*, 419.
- (11) Rozanska, X.; Chipot, C. *J. Chem. Phys.* **2000**, *112*, 9691.
- (12) Masunov, A.; Lazaridis, T. *J. Am. Chem. Soc.* **2003**, *125*, 1722.
- (13) Maksimiak, K.; Rodziewicz-Motowidlo, S.; Czaplowski, C.; Liwo, A.; Scheraga, H. A. *J. Phys. Chem. B* **2003**, *107*, 13496.
- (14) Martorana, V.; La Fata, L.; Bulone, D.; San Biagio, P. L. *Chem. Phys. Lett.* **2000**, *329*, 221.
- (15) Kovalenko, A.; Hirata, F. *J. Chem. Phys.* **2000**, *112*, 10391.
- (16) Soetens, J. C.; Millot, C.; Chipot, C.; Jansen, G.; Angyan, J. G.; Maigret, B. *J. Phys. Chem. B* **1997**, *101*, 10910.
- (17) Pratt, L. R.; Hummer, G.; Garcia, A. E. *Biophys. Chem.* **1994**, *51*, 147.
- (18) Hummer, G.; Soumpasis, D. M.; Neumann, M. *Mol. Phys.* **1994**, *81*, 1155.
- (19) Dang, L. X. *Chem. Phys. Lett.* **1992**, *200*, 21.
- (20) Dang, L. X.; Pettitt, B. M.; Rossky, P. J. *J. Chem. Phys.* **1992**, *96*, 4046.
- (21) Boudon, S.; Wipff, G.; Maigret, B. *J. Phys. Chem.* **1990**, *94*, 6056.
- (22) Yu, H. A.; Roux, B.; Karplus, M. *J. Chem. Phys.* **1990**, *92*, 5020.
- (23) Buckner, J. K.; Jorgensen, W. L. *J. Am. Chem. Soc.* **1989**, *111*, 2507.
- (24) Dang, L. X.; Pettitt, B. M. *J. Am. Chem. Soc.* **1987**, *109*, 5531.
- (25) Pettitt, B. M.; Rossky, P. J. *J. Chem. Phys.* **1986**, *84*, 5836.
- (26) Jeffrey, G. A. *An Introduction to Hydrogen Bonding*; Oxford University Press: Oxford, 1997.
- (27) Hobza, P.; Zahradnik, R. *Chem. Rev.* **1988**, *88*, 871.
- (28) *Water: A Comprehensive Treatise*; Franks, F., Ed.; Plenum Press: New York, 1972–80; Vols. 1–7.
- (29) Vorobjev, Y. N.; Hermans, J. *J. Phys. Chem. B* **1999**, *103*, 10234.
- (30) Zhong, E. C.; Friedman, H. L. *J. Phys. Chem.* **1988**, *92*, 1685.
- (31) Jorgensen, W. L.; Chandrasekhar, J.; Madura, J. D.; Impey, R. W.; Klein, M. L. *J. Chem. Phys.* **1983**, *79*, 926.
- (32) de Leeuw, S. W.; Perram, J. W.; Smith, E. R. *Proc. R. Soc. London, Ser. A* **1980**, *373*, 27.
- (33) de Leeuw, S. W.; Perram, J. W.; Smith, E. R. *Proc. R. Soc. London, Ser. A* **1980**, *373*, 57.
- (34) Darden, T.; York, D.; Pedersen, L. *J. Chem. Phys.* **1993**, *98*, 10089.
- (35) Cheatham, T. E., III; Miller, J. L.; Fox, T.; Darden, T. A.; Kollman, P. A. *J. Am. Chem. Soc.* **1995**, *117*, 4193.
- (36) Essmann, U.; Perera, L.; Berkowitz, M. L.; Darden, T.; Lee, H.; Pedersen, L. G. *J. Chem. Phys.* **1995**, *103*, 8577.
- (37) Bogusz, S.; Cheatham, T. E.; Brooks, B. R. *J. Chem. Phys.* **1998**, *108*, 7070.
- (38) Sagui, C.; Darden, T. *Annu. Rev. Biophys. Biomol. Struct.* **1999**, *28*, 155.
- (39) Hassan, S. A.; Guarnieri, F.; Mehler, E. L. *J. Phys. Chem. B* **2000**, *104*, 6478.
- (40) Hassan, S. A.; Guarnieri, F.; Mehler, E. L. *J. Phys. Chem. B* **2000**, *104*, 6490.
- (41) Hassan, S. A.; Mehler, E. L. *Proteins* **2002**, *47*, 45.
- (42) Hassan, S. A.; Mehler, E. L.; Zhang, D.; Weinstein, H. *Proteins* **2003**, *51*, 109.
- (43) McQuarrie, D. A. *Statistical Mechanics*; Harper & Row: New York, 1976.
- (44) Torrie, G. M.; Valleau, J. P. *J. Comput. Phys.* **1977**, *23*, 187.
- (45) Torrie, G. M.; Valleau, J. P. *J. Chem. Phys.* **1977**, *66*, 1402.
- (46) Paine, G. H.; Scheraga, H. A. *Biopolymers* **1985**, *24*, 1391.
- (47) Mezei, M. *J. Comput. Phys.* **1987**, *68*, 237.
- (48) Straatsma, T. P.; McCammon, J. A. *Annu. Rev. Phys. Chem.* **1992**, *43*, 407.
- (49) Mezei, M.; Ben-Naim, A. *J. Chem. Phys.* **1990**, *92*, 1359.
- (50) McDonald, I. R.; Rasaiah, J. C. *Chem. Phys. Lett.* **1975**, *34*, 382.
- (51) Watanabe, K.; Andersen, H. C. *J. Phys. Chem.* **1986**, *90*, 795.
- (52) Kumar, S.; Bouzida, D.; Swendsen, R. H.; Kollman, P. A.; Rosenberg, J. M. *J. Comput. Chem.* **1992**, *13*, 1011.
- (53) Brooks, B. R.; Bruccoleri, R. E.; Olafson, B. D.; States, D. J.; Swaminathan, S.; Karplus, M. *J. Comput. Chem.* **1983**, *4*, 187.
- (54) Fülischer, M. P.; Mehler, E. L. *Chem. Phys.* **1996**, *204*, 403.
- (55) Mehler, E. L. Ab Initio Approaches for Modeling Intermolecular Interactions and Environmental Effects. In *New Challenges in Computational Quantum Chemistry*; Broer, R., Aerts, P. J. C., Bagus, P. S., Eds.; Drukkerij Van Denderen B. V.: Groningen, 1994; p 85.
- (56) MacKerell, A. D.; Bashford, D.; Bellott, M.; Dunbrack, R. L.; Evanseck, J. D.; Field, M. J.; Fischer, S.; Gao, J.; Guo, H.; Ha, S.; Joseph-McCarthy, D.; Kuchnir, L.; Kuczera, K.; Lau, F. T. K.; Mattos, C.; Michnick, S.; Ngo, T.; Nguyen, D. T.; Prodhom, B.; Reiher, W. E.; Roux, B.; Schlenkrich, M.; Smith, J. C.; Stote, R.; Straub, J.; Watanabe, M.; Wiorkiewicz-Kuczera, J.; Yin, D.; Karplus, M. *J. Phys. Chem. B* **1998**, *102*, 3586.
- (57) Dufner, H.; Kast, S. M.; Brickmann, J.; Schlenkrich, M. *J. Comput. Chem.* **1997**, *18*, 660.
- (58) Feller, S. E.; Pastor, R. W.; Rojnuckarin, A.; Bogusz, S.; Brooks, B. R. *J. Phys. Chem.* **1996**, *100*, 17011.
- (59) Lesser, G. J.; Rose, G. D. *Proteins* **1990**, *8*, 6.
- (60) Pace, C. N. *Biochemistry* **2001**, *40*, 310.
- (61) Pace, C. N. Evaluating contribution of hydrogen bonding and hydrophobic bonding to protein folding. In *Energetics of Biological Macromolecules*; Methods in Enzymology Series; Elsevier: New York, 1995; Vol. 259, p 538.
- (62) Honig, B.; Cohen, F. E. *Folding Des.* **1996**, *1*, R17.
- (63) Nicholls, A.; Sharp, K. A.; Honig, B. *Proteins* **1991**, *11*, 281.
- (64) Hebert, E. J.; Giletto, A.; Sevcik, J.; Urbanikova, L.; Wilson, K. S.; Dauter, Z.; Pace, C. N. *Biochemistry* **1998**, *37*, 16192.
- (65) Jackson, J. D. *Classical Electrodynamics*, 2nd ed.; Wiley: New York, 1975.
- (66) Ehrenson, S. J. *Comput. Chem.* **1981**, *2*, 41.
- (67) Lazaridis, T.; Karplus, M. *Proteins* **1999**, *35*, 133.
- (68) Honig, B.; Nicholls, A. *Science* **1995**, *268*, 1144.
- (69) Sharp, K. A.; Honig, B. *Annu. Rev. Biophys. Biophys. Chem.* **1990**, *19*, 301.
- (70) Warshel, A.; Aqvist, J. *Annu. Rev. Biophys. Biophys. Chem.* **1991**, *20*, 267.
- (71) Chothia, C. *Nature* **1974**, *248*, 338.
- (72) Baldwin, R. L. *Science* **2002**, *295*, 1657.

- (73) Fersht, A. R.; Shi, J.-P.; Knill-Jones, J.; Lowe, D. M.; Wilkinson, A. J.; Blow, D. M.; Brick, P.; Carter, P.; Waye, M. M.; Winter, G. *Nature* **1985**, *314*, 235.
- (74) Papazyan, A.; Warshel, A. *J. Phys. Chem. B* **1997**, *101*, 11254.
- (75) Mehler, E. L.; Warshel, A. *Proteins* **2000**, *40*, 1.
- (76) Chandler, D. *Nature* **2002**, *417*, 491.
- (77) Lum, K.; Chandler, D.; Weeks, J. D. *J. Phys. Chem. B* **1999**, *103*, 4570.
- (78) Dill, K. A. *Science* **1990**, *250*, 297.
- (79) Ben-Naim, A. *Hydrophobic Interactions*; Plenum Press: New York, 1980.
- (80) Hummer, G.; Garde, S.; Garcia, A. E.; Pratt, E. A. *Chem. Phys.* **2000**, *258*, 349.
- (81) Pace, C. N.; Horn, G.; Hebert, E. J.; Bechert, J.; Shaw, K.; Urbanikova, L.; Scholtz, J. M.; Sevcik, J. *J. Mol. Biol.* **2001**, *312*, 393.
- (82) Takano, K.; Scholtz, J. M.; Sacchettini, J. C.; Pace, C. N. *J. Biol. Chem.* **2003**, *278*, 31790.
- (83) Debye, P. *Polar Molecules*; Dover: New York, 1929.
- (84) Lorentz, H. A. *Theory of Electrons*; Dover: New York, 1952.
- (85) Sack, V. H. *Phys. Z.* **1926**, *27*, 206.
- (86) Sack, V. H. *Phys. Z.* **1927**, *28*, 199.
- (87) Ehrenson, S. *J. Comput. Chem.* **1989**, *10*, 77.
- (88) Onsager, L. *J. Am. Chem. Soc.* **1936**, *58*, 1486.
- (89) Li, X. F.; Hassan, S. A.; Mehler, E. L. Submitted for publication, 2004.
- (90) Fukunishi, Y.; Suzuki, M. *J. Phys. Chem.* **1996**, *100*, 5634.